

CHEMISTRY

A European Journal

A Journal of



Accepted Article

Title: Ultrasonic Assisted Linker Exchange (USALE): A Novel Post-Synthesis Method for Controlling the Functionality, Porosity and Morphology of the MOFs

Authors: Ali Morsali and Sayed Ali Akbar Razavi

This manuscript has been accepted after peer review and appears as an Accepted Article online prior to editing, proofing, and formal publication of the final Version of Record (VoR). This work is currently citable by using the Digital Object Identifier (DOI) given below. The VoR will be published online in Early View as soon as possible and may be different to this Accepted Article as a result of editing. Readers should obtain the VoR from the journal website shown below when it is published to ensure accuracy of information. The authors are responsible for the content of this Accepted Article.

To be cited as: *Chem. Eur. J.* 10.1002/chem.201901554

Link to VoR: <http://dx.doi.org/10.1002/chem.201901554>

Supported by
ACES

WILEY-VCH

Ultrasonic Assisted Linker Exchange (USALE): A Novel Post-Synthesis Method for Controlling the Functionality, Porosity and Morphology of the MOFs

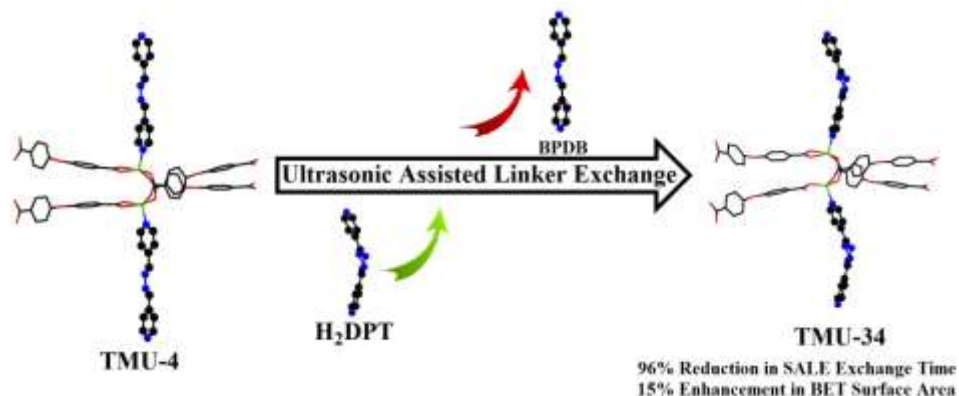
Sayed Ali Akbar Razavi, Ali Morsali*

Department of Chemistry, Faculty of Sciences, Tarbiat Modares University, Tehran, Islamic Republic of Iran. P.O. Box 14117-13116

*E-mail: morsali_a@modares.ac.ir, Tel: (+98) 21-82884416.

Accepted Manuscript

Table of Content



In this work a novel method (ultrasonic assisted linker exchange (USALE)) related to fast and efficient linker substitution had been described which is very quick compared to solvent assisted linker exchange (SALE) method. Moreover, the increased amounts of surface area and pore volume are higher rather SALE, too.

Abstract

Introduction of organic ligands into the metal-organic frameworks (MOFs) structure with specific topology and those that are unattainable through direct synthesis is a big challenge. To solve this challenge different ligand exchange/incorporation methods had been applied. Here, a new method called ultrasonic assisted linker exchange (USALE) introduced to solve mentioned problem. USALE is novel method for ligand exchange based on the use of ultrasonic waves. The temperature and pressure caused by USALE method in microscopic levels are so intense that the linker exchange process is much faster than other methods. In addition to time saving during synthesis method, the use of USALE method leads to higher surface area and pore volume rather other methods like SALE. This observation leads to improved gas adsorption capacity for daughter frameworks synthesized by USALE method. Using USALE method, we transform one of non-porous and easy to synthesis TMU-frameworks ($[\text{Zn}(\text{OBA})(\text{BPDB})_{0.5}]_n \cdot 2\text{DMF}$ (TMU-4) where $\text{H}_2\text{OBA} = 4,4'$ -oxybis(benzoic acid) and $\text{BPDB} = 1,4$ -bis(4-pyridyl)-2,3-diaza-1,3-butadiene) into another porous framework that requires relatively long time to synthesis ($[\text{Zn}(\text{OBA})(\text{H}_2\text{DPT})_{0.5}]_n \cdot \text{DMF}$ (TMU-34) where $\text{H}_2\text{DPT} = 3,6$ -Di(pyridin-4-yl)-1,4-dihydro-1,2,4,5-tetrazine). In addition to reduced synthesis time for TMU-34 (in comparison with both direct sonochemical synthesis and indirect SALE method), the achieved data reveal that USALE synthesized daughter TMU-34 framework has higher surface area and accessible pore volume rather than direct and SALE synthesized TMU-34 frameworks. Application of SALE-TMU-34 and USALE-TMU-34 in catalytic Henry condensation and conformed adsorption show that higher porosity of USALE-TMU-34 leads to higher turn-over frequency and saturation capacity of the USALE-TMU-34 rather SALE-TMU-34.

1. Introduction

Owing to their permanent porosity and three dimensional (3D) crystalline and modular structure, metal-organic frameworks applied enormously in synthesis of materials with tuned and tailored characters.^[1] MOFs extensively applied in different types of applications such as catalyst and photocatalyst,^[2] removal, detection, separation and degradation of pollutants,^[3] gas storage and separation,^[4] construction of electrochemical and electronic devices,^[5] bio application, drug delivery^[6] and magnetic materials.^[7] Such widespread applications of MOFs has taken place due to their unique properties such as high surface area and porosity, thermal and chemical stability, chemically decorable nature, hybrid inorganic-organic nature and mild synthesis conditions.

MOFs had been synthesized using different methods such as conventional solvothermal, microwave, mechanochemical, electrochemical and sonochemical.^[8] Among these methods sonochemical method is of importance because: (I) it is a green synthesis method to develop MOFs,^[9] (II) owing to its nature this method is very fast compared to conventional methods^[10] and (III) nano-sized MOF structures can be obtained using sonochemical method with ability to control the size and morphology of the MOF particles.^[10b, 11] In comparison with conventional energy sources, ultrasonic irradiation provides rather unusual but useful and helpful reaction conditions (a short duration of extremely high temperatures and pressures in liquids) which cannot be provided by other MOF-synthesis methods. Sonochemistry and sonochemical synthesis methods are based on acoustic cavitation which is the major physical phenomenon to affect on a system in ultrasonic bath.^[9, 12] Acoustic cavitation is consist of formation, growth, and implosive collapse of bubbles in a liquid which leads to unleashing the concentrated energy stored inside the bubble within a very short time (with a heating and cooling rate of $>10^{10}$ K.s⁻¹).^[13] Such bubble explosion leads to a temperature of ~5000 K and a pressure of ~1000 bar in microscopic levels in the sonicated solution.^[13]

Unfortunately although there are different methods for synthesizing MOFs, but direct synthesis of MOFs with desirable function–structure properties is not always reliable because of some reasons like formation of undesirable topologies, low solubility of building blocks, and loss of functionality of the sensitive frameworks when synthesizing.^[14] So, to overcome this problem some new synthesis methods must be applied by using pre-synthesized frameworks. Solvent-

assisted linker exchange (SALE) and solvent-assisted ligand incorporation (SALI) are among the well-known and mostly applied method to overcome mentioned challenges.^[14-15] These methods are a kind of similar to conventional direct synthesis of MOFs in term of synthesis conditions. For example in SALE and conventional synthesis method, the reactants should be placed in suitable solvent in an oven and then give the reaction solution a relatively long time (from days to weeks) to make the desirable reaction. This limitation in reaction time encouraged us to seek for a new method for ligand exchange reactions.

Since ultrasonic synthesis of MOFs is a green and time-saving method during direct synthesis of MOF powders, we applied ultrasonication method for fast, time-saving and green ligand exchange procedure. So, we applied ultrasonic assisted linker exchange (USALE) method to solve mentioned problems. The driving force for ligand exchange in USALE method provides by using of ultrasonic waves. In this work, we transformed non-porous and easy to synthesize mother TMU-4 framework (with formula $[\text{Zn}(\text{OBA})(\text{BPDB})_{0.5}]_n \cdot 2\text{DMF}$ where $\text{H}_2\text{OBA} = 4,4'$ -oxybis(benzoic acid) and $\text{BPDB} = 1,4$ -bis(4-pyridyl)-2,3-diaza-1,3-butadiene) framework to porous and easy to synthesize daughter TMU-34 frameworks ($[\text{Zn}(\text{OBA})(\text{H}_2\text{DPT})_{0.5}]_n \cdot \text{DMF}$ where $\text{H}_2\text{DPT} = 3,6$ -Di(pyridin-4-yl)-1,4-dihydro-1,2,4,5-tetrazine). Achieved results show that USALE-synthesized TMU-34 (USALE-TMU-34) has higher surface area, higher accessible pore volume and higher N_2 (at 77 K) and CO_2 (at 298 K) adsorption capacity rather SALE-synthesized (SALE-TMU-34) and direct-sonochemical synthesized TMU-34 samples. Also, owing to higher porosity, USALE-synthesized TMU-34 remove larger amount of congo-red from aqueous solution and reaches maximum conversion (%) in Henry condensation in relatively shorter times owing to higher porosity and more comfortable diffusion of substrates into the pores.

2. Experimental

2.1. Chemical and methods

Materials. All required chemicals were purchased from commercial suppliers and were used without further purification unless otherwise noted. Especially, (4,4'-oxybis(benzoic acid)) H_2OBA was purchased from Aldrich company.

Instrumentation. Ultrasonication was carried out in a Sonica-2200 EP ultrasonic bath (frequency 40 KHz). X-ray powder diffraction (XRD) measurements were performed using a Philips X'pert diffractometer with monochromated Cu-K α radiation. Elemental analyses were carried out on a Thermo Scientific Flash 2000 CHNS elemental analyzer. Adsorption studies were performed using a TriStar II 3020 surface area analyzer from Micromeritics Instrument Corporation with N $_2$ at 77 K and CO $_2$ at 298 K. UV-Vis absorbance spectra were measured on a Varian Cary 50 UV-Vis spectrophotometer equipped with a single-beam facility with a spectral resolution of 0.2 nm. Luminescence spectra were recorded with a PerkinElmer LS-55 fluorescence spectrometer at room temperature. Infrared spectra were recorded using Thermo Nicolet IR 100 FT-IR. Thermal behavior was measured with a PL-STA 1500 apparatus at a rate of 10 °C.min $^{-1}$ under a static atmosphere of nitrogen. ^1H NMR spectra were recorded on a Bruker 500 NMR spectrometer. The samples were characterized with a scanning electron microscope (SEM) ZEISS SIGMA VP (Germany) with gold coating.

2.2. Synthesis of pillars and frameworks

Synthesis of pillar spacers. 3,6-Di(pyridin-4-yl)-1,4-dihydro-1,2,4,5-tetrazine (H $_2$ DPT) and 1,4-bis(4-pyridyl)-2,3-diaza-1,3-butadiene (BPDB), used as spacers, were synthesized according to the techniques reported previously.^[4d, 16]

Synthesis of TMU-4. The mixture of H $_2$ OBA (0.128 g, 0.5 mmol), BPDB (0.105 g, 0.5 mmol) and Zn(CH $_3$ COO) $_2$ ·2H $_2$ O (0.07 g, 0.3 mmol) in 20 mL DMF were ultrasonicated in an ultrasonic bath at ambient temperature and atmospheric pressure for 60 min. The resulting yellow powder was isolated by centrifugation, washed with DMF three times and dried at 80°C. Yield: 83%. IR data (KBr pellet, cm $^{-1}$): selected bands: 445(w), 523(w), 659(m), 692(m), 776(m), 875(m), 1021(w), 1089(m), 1159 (s), 1241(vs), 1389(vs), 1412(vs), 1500(s), 1568(s), 1608(vs), 1679(vs), 2926(w) and 3414(w-br). Elemental analysis (%) calculated for [Zn(C $_{14}$ O $_5$ H $_8$)(C $_{12}$ H $_{10}$ N $_4$) $_{0.5}$](C $_3$ NOH $_7$) $_2$: C: 55.3, H: 4.0, N: 8.4; Found: C: 55.8, H: 4.2, N: 8.5.2.5

Synthesis of TMU-34. TMU-34 powder was synthesized from a mixture of Zn(CH $_3$ COO) $_2$ ·2H $_2$ O (0.22 g, 1 mmol), H $_2$ OBA (0.26 g, 1 mmol), and H $_2$ DPT (0.24 g, 1 mmol) in DMF (30 mL). The mixture was sonicated for 160 min at ambient temperature and atmospheric pressure. It was then centrifuged and the resulting powder was washed with DMF

and dried at room temperature. Yield: 0.34 g (78% based on OBA). IR (KBr pellet, cm^{-1}): selected bands: 661 (m), 778 (m), 872 (m), 1162 (s), 1241 (vs), 1407 (vs), 1607 (vs), 1674 (s), 2928 (m), 3273; Elemental analysis (%) calculated for $[\text{Zn}(\text{C}_{14}\text{O}_5\text{H}_8)(\text{C}_{12}\text{N}_6\text{H}_{10})_{0.5}] \cdot (\text{C}_3\text{ONH}_7)$: C 53.8, N 10.9, H 3.9; found: C 54.1, N 11.4, H 4.1.

2.3. Linker exchange procedures

For transformation of non-porous and easy to synthesize mother TMU-4 framework to daughter TMU-34 frameworks, SALE and novel USALE linker exchange method had been performed.

Solvent assisted linker exchange (SALE). A number of 10 ml screw cap glass vial was used for SALE procedure. 0.3 g activated TMU-4 added to each one of glass vials and followed by addition of 10 ml H_2DPT ligand solution which had been prepared by dissolution of 1 g H_2DPT in 100 mL of DMF (10 $\text{g}\cdot\text{L}^{-1}$ ligand solution). Sampling for monitoring the exchange process was carried out at intervals of every 12 hours until the ligand exchange is complete (0, 12, 24, 36, 52 hours). Exchange procedure monitored using ^1H NMR and photoluminescence spectroscopy techniques.

Ultrasonic assisted linker exchange (USALE). The general condition for USALE is same as SALE procedure, but monitoring the exchange process was carried out at intervals of every 30 minutes (0, 30, 60, 90 and 120 minutes). Exchange procedure monitored using ^1H NMR and photoluminescence spectroscopies.

2.4. General procedure for Henry condensation.

To examine the roles of porosity and functionality of synthesized frameworks, TMU-4, TMU-34, SALE-TMU-34 and USALE-TMU-34, Henry condensation had been conducted. All samples activated before catalytic tests as reported procedure.^[4d]

A 6 ml screw cap glass vial with magnetic stir bar was used to carry out the catalytic test reaction. 0.03 g of activated frameworks (0.034 mmol of catalytic sites and 1.7 mol% of catalyst) added to the glass vial and followed by addition of 5 ml aqueous solution of benzaldehyde (5 mmol, excess reagent) and nitromethane (2 mmol, limiting reagent). The mixture stirred at 60 °C and atmospheric pressure for 10 hour. Then the catalyst and solution separated by centrifugation (6000 rpm). The catalyst dried and applied for XRD and N_2 adsorption analysis. The above

filtrate solution applied for GC analysis to calculate the catalytic reaction conversion (%). Recyclability test conducted for 5 times in the same procedure.

2.5. General procedure for dye adsorption.

For evaluation the roles of porosity and functionality of synthesized frameworks, TMU-4, TMU-34, SALE-TMU-34 and USALE-TMU-34, dye adsorption experiment had been conducted. Here, all samples activated before adsorption tests, too. 100 ppm solution of congo-red (CR) was chosen as a model pollutant solution to evaluate the adsorption capacity of the frameworks. CR adsorption experiments were carried out in an ultrasonic bath in different volumes in the presence of 50 mg activated frameworks at ambient conditions and sonicated for 10 minutes. Small portion of samples for UV-Vis analyses were taken from the suspension at specified time intervals (0, 5, 10, 15, 20, 25, 30, 35, 40, 45, 50, 60, 70, 80, 90 minutes) to monitor adsorption process by UV-Vis analysis.

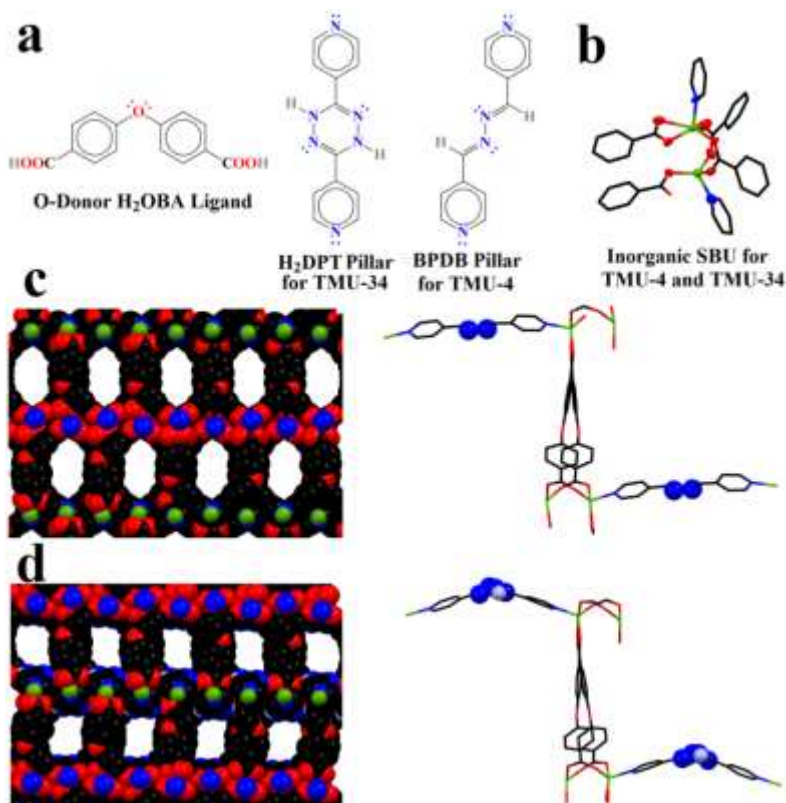
3. Results and Discussion

3.1. Synthesis and Characterization

Here, ultrasonication method had been applied for both direct-synthesis and post-synthesis of MOFs. TMU-4 and TMU-34 had been directly synthesized by sonochemical method using $\text{Zn}(\text{CH}_3\text{COO})_2 \cdot 2\text{H}_2\text{O}$, H_2OBA and related pillar spacers; BPDB for TMU-4 and H_2DPT for TMU-34. PXRD patterns show that direct sonochemical synthesized TMU-4 and TMU-34 have same PXRD pattern as their simulated and crystalline structure (**Figure S1**). As a nonporous (toward N_2) and easy-to-synthesis mother framework, TMU-4 applied in SALE and USALE methods to become converted into the SALE-TMU-34 and USALE-TMU-34 daughter frameworks using a solution of H_2DPT in DMF ($\text{N,N}'$ -dimethylformamide).

3D structure of pillar-layered TMU-4 framework is developed based on linking of 2D sheets by BPDB N-donor pillar spacer. 2D sheets are constructed by deprotonation of H_2OBA and coordination of free carboxylate groups of OBA^{2-} to Zn^{2+} metal ions to generate non-symmetrical $\text{Zn}\#1$ - $\text{Zn}\#2$ secondary building blocks with distorted tetrahedral and square-planar geometries. TMU-34 is containing of azine decorated 1D pores with $10.8 \times 10.7 \text{ \AA}$ theoretical maximum open pore size (TMOPS) based on crystallographic data (**Scheme 1**). Similarly, TMU-

34 is based on H₂OBA, H₂DPT and Zn²⁺ building blocks, Zn₂(COO)₂ 2D sheets with non-symmetrical Zn#1-Zn#2 secondary building blocks, 3D pillar layered structure by H₂DPT and dihydro-tetrazine decorated 1D pores with 10.8 × 10.5 Å TMOPS (**Scheme 1**).



Scheme 1. Structural representation of TMU-frameworks. (a) molecular structure of O and N-donor ligands. (b) Non-symmetrical Zn#1-Zn#2 secondary building blocks (Zn₂(COO)₂). (c) One-dimensional azine decorated pores of TMU-4. (d) One-dimensional dihydro-tetrazine decorated pores of TMU-34.

Although TMU-4 and TMU-34 are isostructure (**Figure S2**) with close structural parameters (**Table S1**), but their differences based on applied N-donor pillar spacers (BPDB for TMU-4 vs. H₂DPT for TMU-34) had led to different properties. In addition to different functionality (azine for TMU-4 vs. dihydro-tetrazine for TMU-34), TMU-4 is non-porous toward N₂ molecules (**Figure 1**) with short sonochemical synthesis time (**Table 1**). Inversely, TMU-34 is porous toward N₂ molecules (**Figure 1**) with relatively long sonochemical synthesis time (**Table 1**).

Despite TMU-4 which is nonporous toward N₂ molecules, TMU-34 shows type I isotherm relating to microporous solids. But, the isotherms for SALE-TMU-34 and USALE-TMU-34 samples differ (**Figure 1**). SALE-TMU-34 and USALE-TMU-34 show type IV isotherms indicating mesoporosity character of the adsorbents (**Figure 1**). Such difference in porosity

nature of direct-synthesized TMU-34 framework and daughter SALE-TMU-34 and USALE-TMU-34 frameworks show that the essences of the created defects in the daughter frameworks after exchange procedures are based on mesoporous nature.

Table 1. Gas adsorption properties of direct and post synthesized frameworks.

	TMU-4	TMU-34	SALE-TMU-34	USALE-TMU-34
N ₂ (cm ³ .g ⁻¹)-77 K	(nonporous)	197	224	243
BET (m ² .g ⁻¹)	-	540	720	830
Pore Volume (cm ³ .g ⁻¹)	-	0.28	0.34	0.38
CO ₂ (cm ³ .g ⁻¹)-298 K	39	30	38	50
Synthesis Time (min)	30	160	3120	120

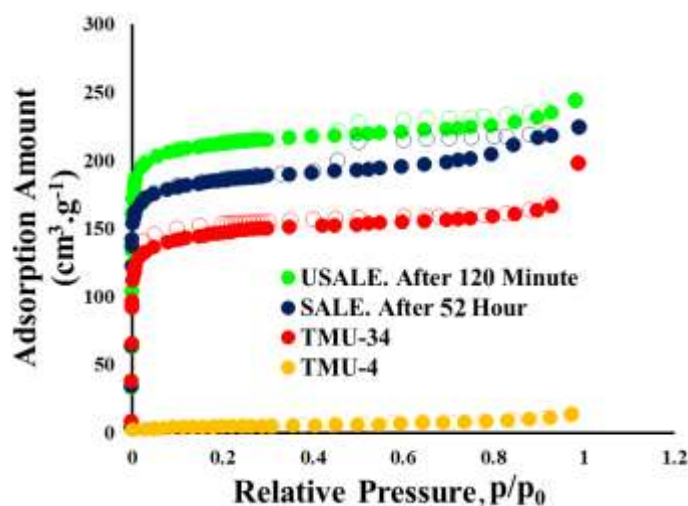


Figure 1. N₂ adsorption properties of direct and post synthesized frameworks.

Scanning electron microscopy (SEM) images show that TMU-4 and TMU-34 represent different morphologies (**Figure 2**). TMU-4 morphology is based on micro-plates with 200-250 nm thickness. But in case of TMU-34, morphology is based on completely aggregated particles without specific shape with thickness varying from several hundred nanometers to several micrometers.

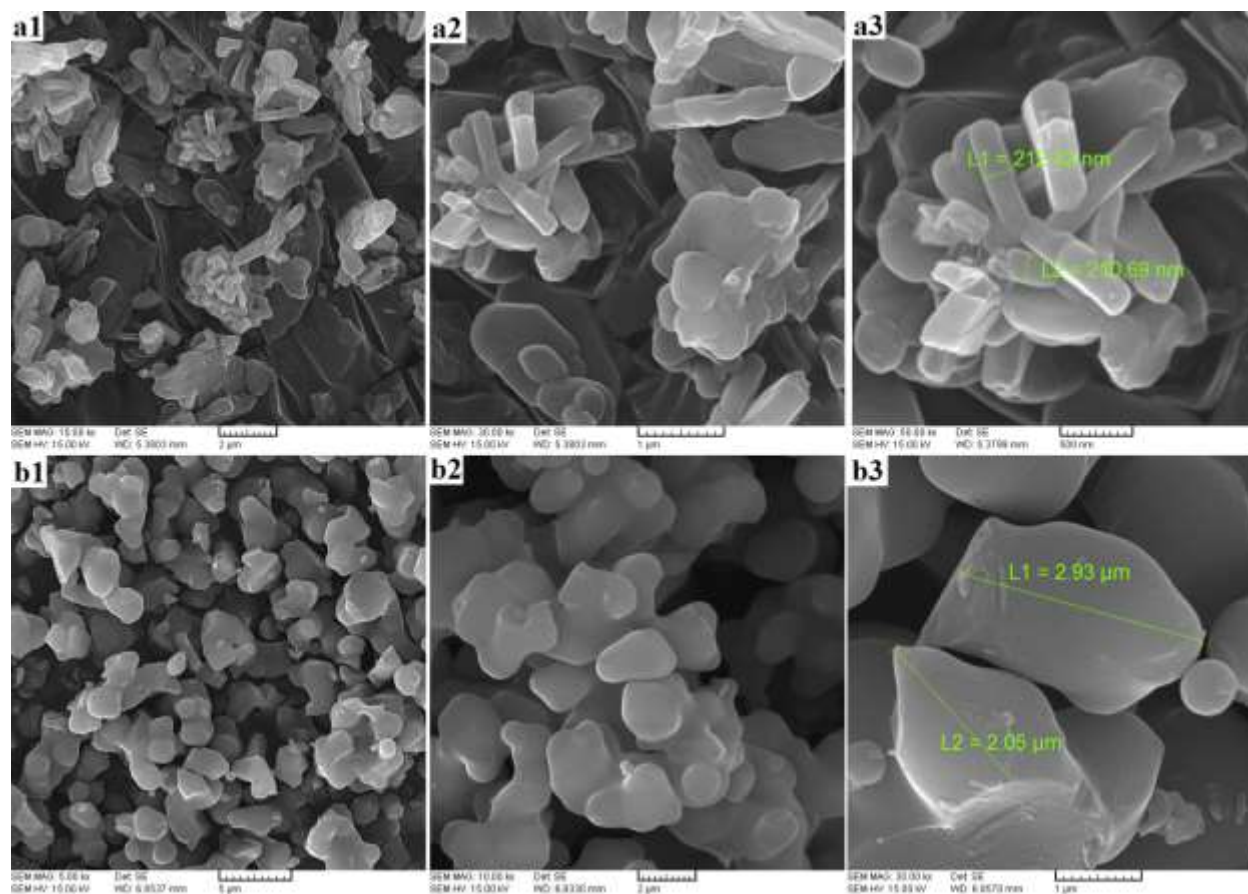


Figure 2. SEM images of TMU-4 (a) and TMU-34 (b).

3.2. Ligand Exchange Procedure

Considering the advantages of TMU-4 (easy and short synthesis time, uniform morphology with smaller particle size) and TMU-34 (porosity toward N_2 and dihydro-tetrazine function efficiency as H-donor^[3e], H-bond donor^[3g] and Lewis basic site^[4d]) frameworks, we tried to combine and improve these beneficial characters into the one framework. So, we used linker exchange methods, solvent-assisted linker exchange (SALE) and ultrasonic-assisted linker exchange (USALE) methods, in a way that TMU-4 applied as parent framework and TMU-34 as targeted daughter framework. According to mentioned procedure in section 2.3, a solution of H_2DPT in DMF was poured on TMU-4 powder and then linker exchange using SALE and USALE methods performed in preheated $120\text{ }^\circ\text{C}$ oven and ultrasonic bath, respectively.

Linker exchange kinetic in both SALE and USALE procedures monitored by $^1\text{H-NMR}$ and photoluminescence spectroscopies. For $^1\text{H-NMR}$ analysis, approximately 5 mg of TMU-4 in

different time intervals was placed in an NMR tube and dissolved in D₂SO₄ (100 mL) and [D₆]DMSO (0.6 mL) with the aid of sonication. Once a homogeneous solution had been obtained, ¹H-NMR spectra were obtained by locking the sample to [D₆]DMSO. Prior to ¹H-NMR, linker exchange treated TMU-4 powder was soaked for 4 h in fresh DMF to remove residual ligands. For PL analysis, approximately 2 mg of TMU-4 in different time intervals had been sonicated for 10 min and once a homogeneous and dispersed solution had been obtained, PL measurement carried out.

Based on ¹H-NMR spectrum, the most distinct differences in TMU-4 and TMU-34 spectrum are according to dihydro-tetrazine (-NH) peak for daughter TMU-34 framework around 9.5 ppm and azine (H-C=N) peak for parent TMU-4 framework around 8.4 ppm (**Figure S3**). Linker exchange procedure by ¹H-NMR technique monitored using these two peaks (**Figure 3**). Sampling for ¹H-NMR had been done at every 30 min for USALE and 12 hour for SALE procedures. According to the ratio of BPDB/H₂DPT pillar spacers (**Table S2**) it is clear that SALE and USALE procedures are completed after 52 hour (3120 min) and 120 min, respectively. The end of exchange procedure, SALE and USALE, is considered at a time when the TMU-4 peak around 8.4 ppm related to (H-N=C) is completely disappeared. It is clear that by continuing the exchange procedure the intensity for TMU-4 peak (~ 8.4 ppm, blue) is reduced and the intensity for TMU-34 peak (~ 9.5 ppm, red) is increased (**Figure 3**).

Since TMU-4 and TMU-34 have different excitation wavelength (338 nm for TMU-4 and 482 nm for TMU-34 in water), emission band (430-520 nm for TMU-4 and 570-675 nm for TMU-34) and maximum emission peak (465 nm for TMU-4 and 615.5 nm for TMU-34), PL measurement is another helpful method to monitor exchange procedure (**Figure S4**). Similar results had been achieved by monitoring the SALE and USALE procedures using PL measurement (**Figure 4**). SALE and USALE procedure became completed after 52 hour (3120 min) and 120 min respectively. H₂DPT/BPDB ratio at every interval time is very close to those achieved by ¹H-NMR method (**Table S3**). The end of exchange procedure, SALE and USALE, is considered at a time when the TMU-4 emission peak band (430-520 nm) had been turned-off completely.

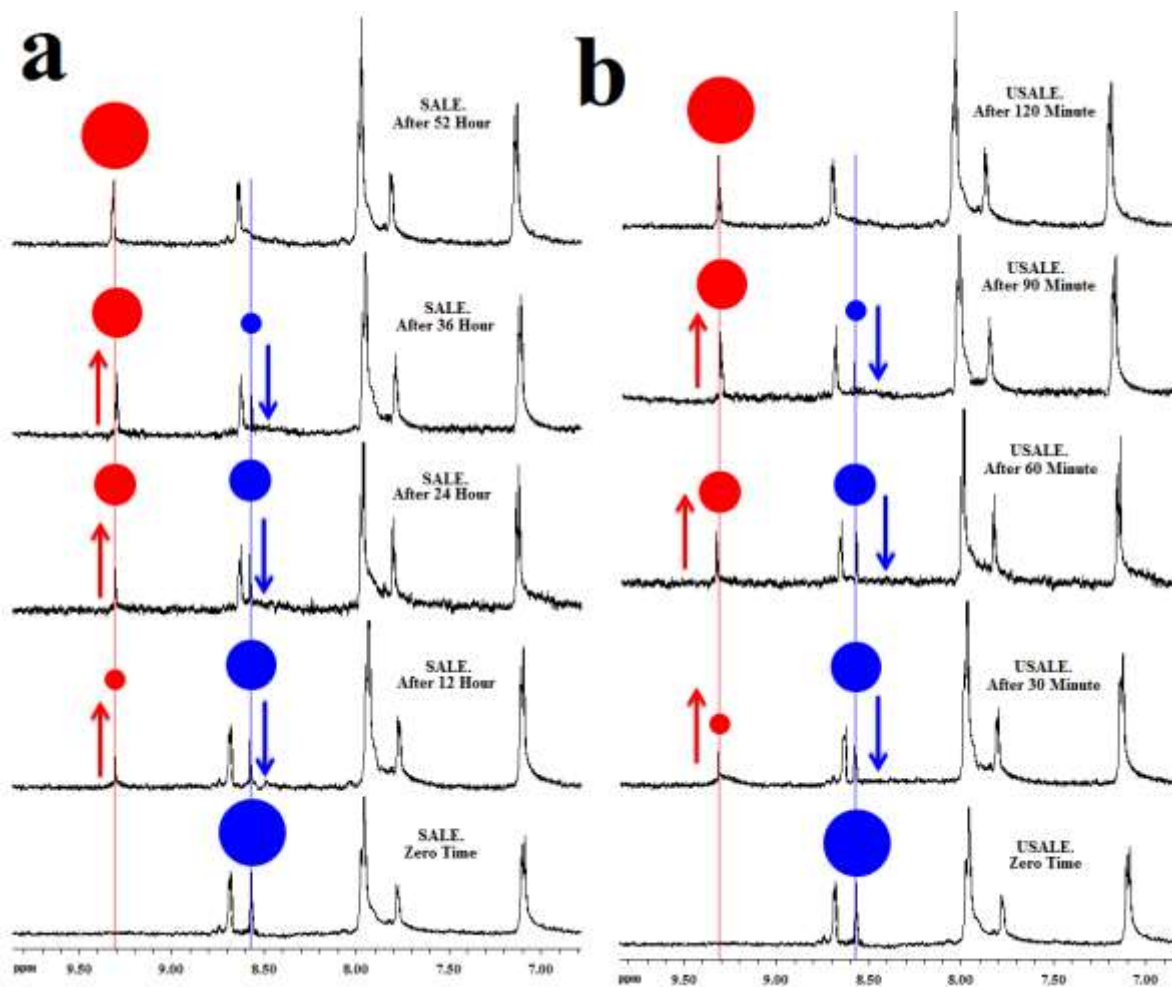


Figure 3. $^1\text{H-NMR}$ spectrum for SALE (a) and USALE (b) procedure.

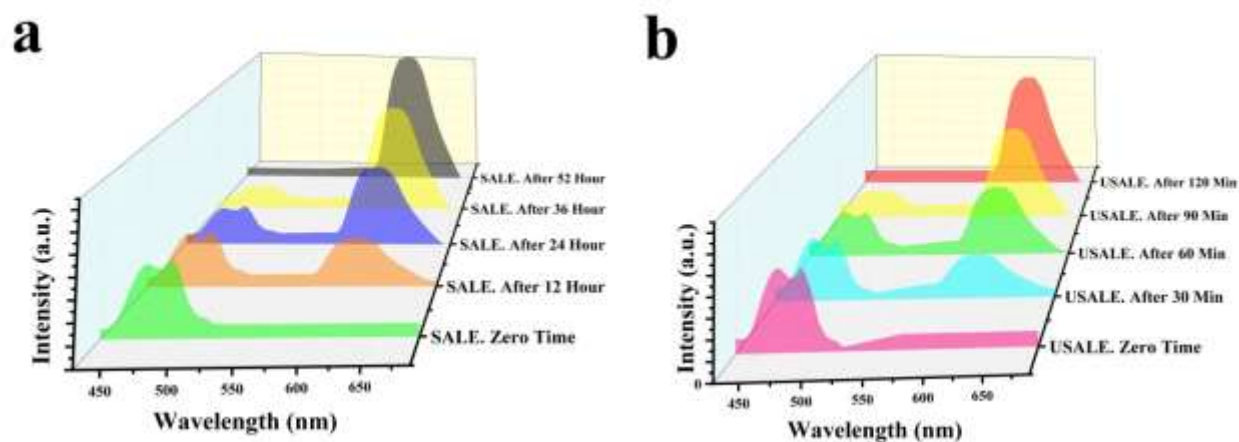


Figure 4. PL emission spectrum for SALE (a) and USALE (b) procedure.

Since parent TMU-4 framework and sonochemically synthesized TMU-34 represent same PXRD patterns, we anticipate that daughter SALE-TMU-34 and USALE-TMU-34 frameworks show same PXRD patterns (**Figure S5**). **Figure 5** compares the synthesized TMU-4, TMU-34, SALE-TMU-34 and USALE-TMU-34.



Figure 5. Synthesized powder of the frameworks and related N-donor ligands. (a) BPDB pillar spacer for construction of TMU-4. (b) As-synthesized powder of TMU-4. (c) H₂DPT pillar spacer for construction of TMU-34. (d) As-synthesized powder of TMU-34. (e) As-synthesized powder of SALE-TMU-34. (f) As-synthesized powder of USALE-TMU-34.

Gas adsorption analysis (N₂ at 77 K and CO₂ at 298 K) had been conducted to evaluate porosity and surface area of daughter SALE-TMU-34 and USALE-TMU-34 frameworks and compare with direct synthesized TMU-4 and TMU-34 frameworks. Interestingly, **Table 1** and **Figure 1** represent that the daughter framework synthesized by USALE method have higher adsorption capacity (cm³.g⁻¹) toward N₂ and CO₂, higher pore volume (cm³.g⁻¹) and surface area (m².g⁻¹). This noticeable difference in adsorption properties and exchange kinetic is related to nature of ligand exchange driving force in SALE and USALE methods. In USALE method, cavitation collapse at the interface of liquid (H₂DPT solution)-solid (TMU-4 parent framework) leads to

faster removing of BPDB ligand from the framework which results in linker-based substantial defects inside the parent framework.^[10a, 13, 17] On the other hand, using ultrasound waves makes the penetration of the H₂DPT ligands inside the frameworks kinetically easier. As results, ligand replacement can be performed more quickly in free spaces created by linker-based substantial defects. This phenomenon allows the exchange of ligands in much less times (120 min for USALE vs. 3120 min for SALE). On the other hand, USALE-TMU-34 framework with improved porosity and adsorption capacity can be synthesized in smaller time even in comparison with direct sonochemically synthesized TMU-34.

It is recognized that: (I) using ultrasonic method in synthesis of nano-materials leads to improved porosity and surface area of targeted materials because of reduction in particle size and defect creator nature of this method^[9, 10b] and (II) using SALE leads to higher surface area and porosity owing to (partial) eliminating the interpenetration and linker-based substantial defects.^[18] So, it make sense that using ultrasonic method in linker exchange process leads to higher surface area for USALE-daughter framework rather SALE synthesized one. Thermogravimetric analysis (TGA) clearly show that USALE-TMU-34 sample carries much more solvent molecules inside the pores rather SALE-TMU-34 sample (6.71% vs. 17.52 in **Figure S6**). As mentioned, USALE-TMU-34 higher porosity and accessible pore volume is owing to partial elimination of 2-fold interpenetration and created linker-based substantial defects during exchange reaction.

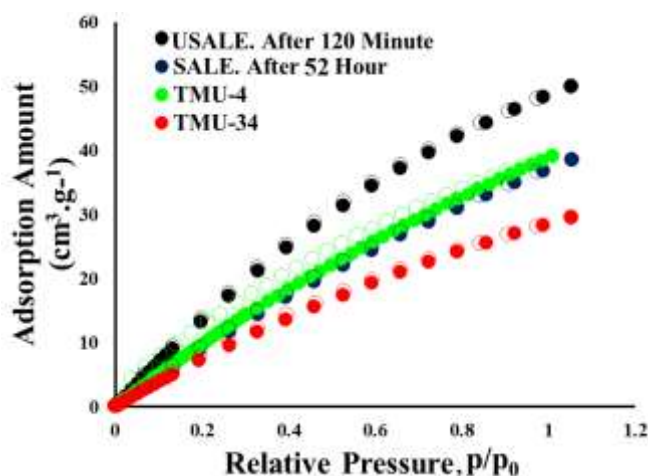


Figure 6. CO₂ adsorption at 298 K.

SEM images display that unlike the sonochemically direct-synthesized TMU-34 sample with aggregated morphology and large particle size, daughter USALE-TMU-34 and SALE-TMU-34 frameworks have uniform micro-plate morphologies. Similar to TMU-4 parent framework, particle thickness for SALE-TMU-34 is mainly in range of 200-250 nm (**Figure 7**). But for USALE-TMU-34 sample particle thickness is mainly lower than 200 nm.

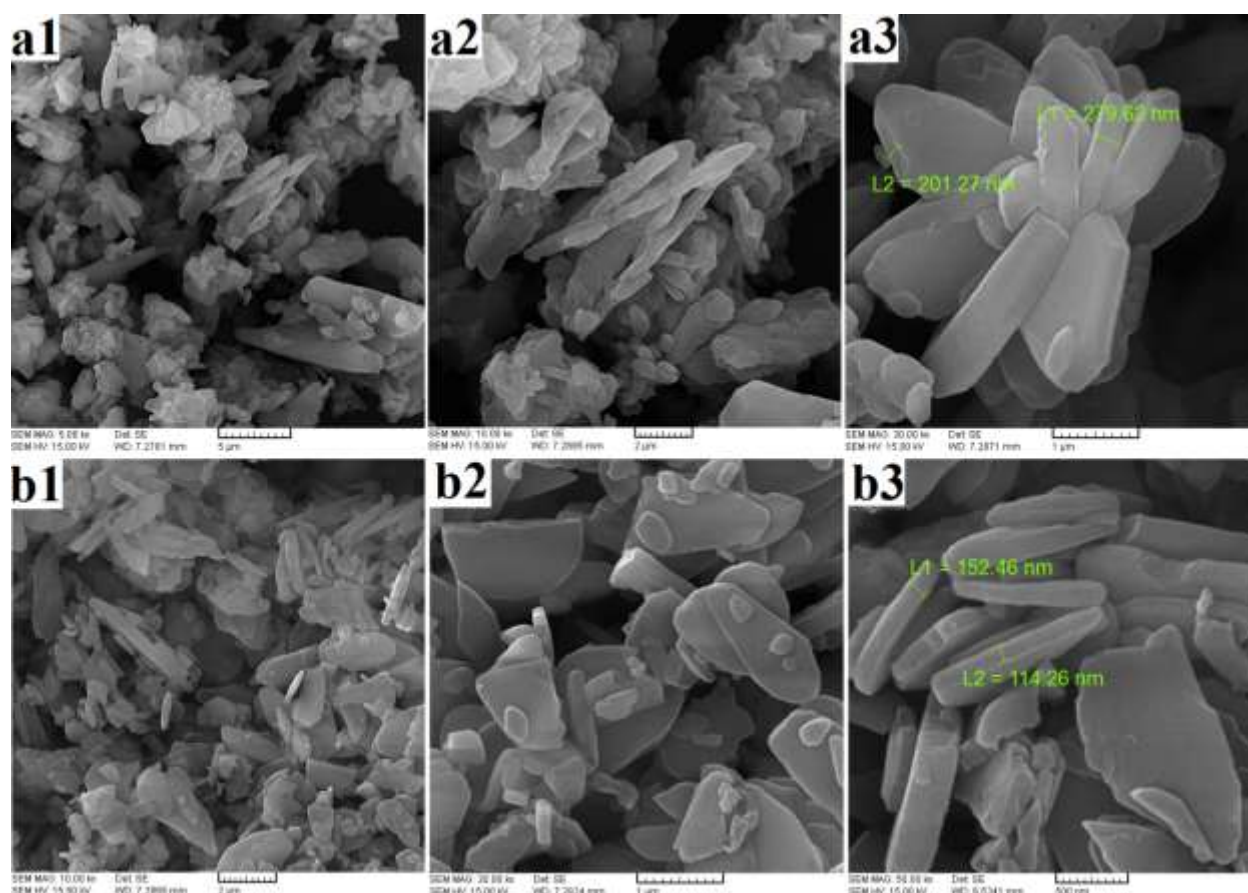


Figure 7. SEM images of SALE-TMU-34 (**a**) and USALE-TMU-34 (**b**) samples.

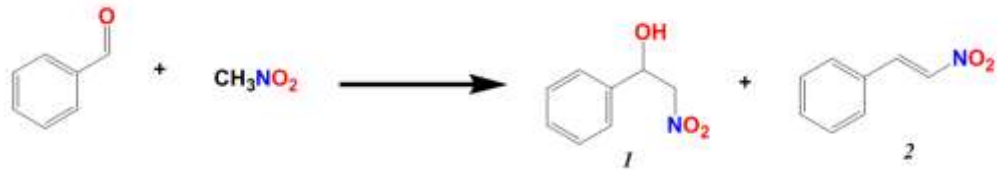
So, our attempt to synthesis of TMU-34 framework with increased porosity, surface area and optimized porosity was successful through synthesis of USALE-TMU-34 sample. Interestingly, USALE-TMU-34 sample can be synthesized in shorter time rather sonochemically direct-synthesized TMU-34 framework (160 min vs. 120 min). Moreover, USALE-TMU-34 sample shows improved properties rather SALE-TMU-34. USALE-TMU-34 show increased porosity and surface area (15%), pore volume (10%) and decreased synthesis time (96%) rather SALE-TMU-34 sample. All these descriptions reveal that USALE is a very effective method for improving the porosity and adsorption capacity as well as optimization of morphology of MOFs.

Since adsorption and catalysis applications are highly depended on the functionality and porosity of the host frameworks, we applied all four frameworks including TMU-4, sonochemically direct-synthesized TMU-34 (TMU-34), daughter SALE-TMU-34 (SALE-TMU-34) and daughter USALE-TMU-34 (USALE-TMU-34) frameworks in nitroaldol condensation and conged removal to evaluate the roles of functionality and improved porosity in mentioned applications.

3.3. Nitroaldol Condensation

Nitroaldol condensation is a reaction between nitroalkane and carbonyl containing α -hydrogen to form new C-C bond between α -carbon of nitroalkane and carbonyl C atom of carbonyl. Nitroaldol condensation can be catalyzed by Lewis basic catalysts. Since all four mentioned frameworks are decorated with Lewis basic organocatalyst sites, azine and dihydro-tetrazine, we conducted this reaction using the TMU-4, TMU-34, SALE-TMU-34, USALE-TMU-34 Lewis basic heterogeneous MOF-based catalysts. In addition to differences in functionality, these four MOFs also differ in porosity and surface area. Such similarities and differences allow to be investigated the role of functionality and porosity of these four frameworks in nitroaldol condensation.

Nitroaldol condensation procedure using TMU-4, TMU-34, SALE-TMU-34 and USALE-TMU-34 had been conducted as reported in section 2.4 and the results are gathered in **Table S4**. The relevant data based on optimized conditions are presented in **Table 2**. Due to the sharp differences in conversion(%) of TMU-4 and other frameworks (more than 4 times), it is possible to decelerate that dihydro-tetrazine function inside the pore-walls of TMU-34, SALE-TMU-34 and USALE-TMU-34 is more effective Lewis basic heterogeneous organocatalyst site rather azine group inside the framework of TMU-4. But there is still a difference between these three structures. Although TMU-34, SALE-TMU-34 and USALE-TMU-34 frameworks are decorated with dihydro-tetrazine function, but they had different porosity and surface area in a way that the catalyst with higher porosity and surface area show higher conversion(%), TON and TOF. This observation can be due to the fact that by increasing the porosity and surface area, more reactant molecules can penetrate inside the framework cavities which act as nano-reactors functionalized with Lewis basic organocatalytic dihydro-tetrazine sites. As a result, the reaction proceeds more rapidly and maximum conversion time can be achieved is shorter time as well as higher TOF and TON numbers.

Table 2. Results of nitroaldol condensation in optimized condensations.*


	BET (m ² .g ⁻¹)	Function	Conversion (%)	Selectivity (%)***	TON****	TOF*****
TMU-4	518**	Azine	20	75	~12	1.2
TMU-34	540	Dihydro-tetrazine	91	82	~54	5.4
SALE-TMU-34	720	Dihydro-tetrazine	95	82	~56	5.6
USALE-TMU-34	830	Dihydro-tetrazine	100	83	~59	5.9

*: Optimized catalytic reaction conditions (0.03 g activated catalyst, stirring at 60 °C, 5cc methanol, 5 mmol benzaldehyde (excess), 2 mmol nitromethane (limited), 10 hour.
 **: Calculated by CO₂ adsorption at 195 K.
 ***: Selectivity toward product 1.
 ****: Turn-over number (= (mmol limited reactant)/(mmol of catalyst))
 *****: Turn-over frequency (ratio of TON over reaction time (hour))

Evaluation of catalytic activity of USALE-TMU-34 as optimized catalysts in filtration test (**Figure S7**), Stability test (**Figure S8**), porosity (**Figure S9**) and reusability test (**Figure S10**) show that presence of USALE-TMU-34 for progressing the nitroaldol reaction is essential and this framework can save its catalytic activity and structural stability and porosity even after 3 cycles.

3.4. Dye Adsorption Experiment

Adsorption capacity of MOF is highly depended to their porosity and surface area and application of TMU-4, TMU-34, SALE-TMU-34 and USALE-TMU-34 in N₂ adsorption clearly show that higher surface area and porosity leads to higher adsorption capacity toward gas molecules. Considering this point, we applied four mentioned framework in adsorption experiments in liquid phase to investigate the ability of these framework in liquid phase. 50 cc of 100 ppm aqueous solution of Congo red was selected as model pollutant for adsorption experiment in gas phase. Here we choose Congo red because: (I) the adsorption capacity of the adsorbent MOFs toward Congo red molecules is dominantly determined by pore volume and surface area^[19] and (II) shape and dimensionality of molecular skeleton of Congo red molecules is suitable for into the 1D pores of the frameworks (**Figure S11**).

Adsorption experiments conducted as section 2.4 and the results are gathered in **Figure S12** and **Table 3**. The results show that the type of functional group does not have much effect on the adsorption process. On the other side, it is easy to understand that increasing the surface area and pore volume will increase the adsorption capacity as well as the time to reach maximum capacity (**Figure 8**). Stability and reusability tests show that USALE-TMU-34 save its capacity, porosity and crystallinity at least after 3 cycles (**Figure S13-S15**)

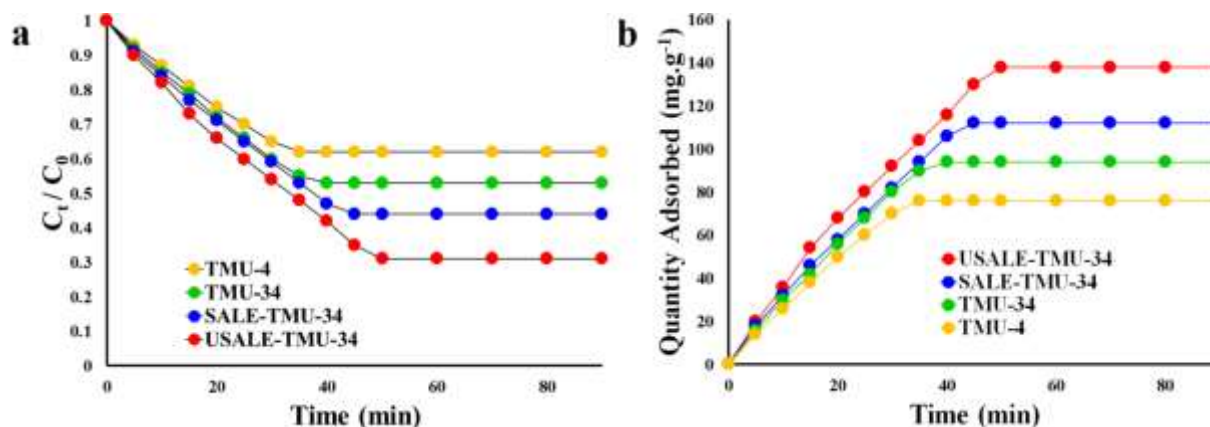


Figure 8. Time-dependent adsorption capacity for TMU-frameworks. (a) Concentration curve. (b) Maximum capacity curve.

Table 3. Congored adsorption data at equilibrium.

	BET ($\text{m}^2\cdot\text{g}^{-1}$)	Function	Removal Efficiency (%)	Maximum Capacity ($\text{mg}\cdot\text{g}^{-1}$)	Equilibrium time (min)
TMU4	518*	Azine	38	72	35
TMU-34	540	Dihydro-tetrazine	47	94	40
SALE-TMU-34	720	Dihydro-tetrazine	56	112	45
USALE-TMU-34	830	Dihydro-tetrazine	69	138	50

*: Calculated by CO_2 adsorption at 195 K.

Finally in this work we show that through ultrasonic-assisted exchange reaction we were able to improve the porosity and surface area of TMU-34 as well as modified morphology and decreasing the particle size. Moreover, the synthesis time had been decreased (25%). Application of USALE-TMU-34 sample with improved surface area in catalytic nitroaldol condensation show that by increasing of the surface area and pore volume of the catalyst, the diffusion rate of the reactants into the Lewis basic decorated pores increase which results in higher number of

TOF factor. Also adsorption capacity in both gas and liquid phase show that by increasing the pore volume, adsorbed amount of N_2 and congored molecules increased.

Conclusion

In this work we synthesized two samples of MOF powders, TMU-4 and TMU-34, by direct sonochemical method for 30 and 160 min, respectively. TMU-4 is an easy to synthesis MOF which nonporous toward N_2 at 77 K along with uniform micro-plate morphology. TMU-34 is porous toward nitrogen at 77 K with aggregated non-uniform morphology with particle size from several hundred nanometers to several micrometers. Since, the only difference in building block of TMU-4 and TMU-34 is related to the N-donor pillar spacers, BPDB for TMU-4 and H_2DPT for TMU-34, we applied linker exchange methods to replace BPDB (inside the parent framework of TMU-4) with H_2DPT (inside the daughter framework of TMU-34) to afford dihydro-tetrazine decorated TMU-34 framework with modified morphology, improved porosity and surface area. We applied SALE and novel USALE methods. Interestingly we observe that USALE method is much more useful rather SALE method in which USALE-TMU-34 sample shows improved properties rather SALE-TMU-34. USALE-TMU-34 show increased porosity and surface area (15%), pore volume (10%) and decreased synthesis time (96%) rather SALE-TMU-34 sample. Also, synthesis time for USALE-TMU-34 is shorter than direct synthesized TMU-34 (120 min vs. 160 min). Application of TMU-34, SALE-TMU-34 and USALE-TMU-34 in catalytic and adsorption experiments show that owing to its functionality and improved porosity, USALE-TMU-34 is more effective that both SALE-TMU-34 and TMU-34. More studies about USALE method are underway.

AUTHOR INFORMATION

Corresponding Authors

*E-mail: morsali_a@modares.ac.ir. Tel: (+98) 21-82884416

ORCID

Ali Morsali: 0000-0002-1828-7287

Notes

The authors declare no competing financial interest.

ACKNOWLEDGMENT

Support of this investigation by Tarbiat Modares University is gratefully acknowledged.

References

- [1] B. Li, H. M. Wen, Y. Cui, W. Zhou, G. Qian and B. Chen, *Advanced Materials* **2016**, *28*, 8819-8860.
- [2] a) J. Liu, L. Chen, H. Cui, J. Zhang, L. Zhang and C.-Y. Su, *Chemical Society Reviews* **2014**, *43*, 6011-6061; b) A. Corma, H. García and F. Llabrés i Xamena, *Chemical reviews* **2010**, *110*, 4606-4655; c) J. Lee, O. K. Farha, J. Roberts, K. A. Scheidt, S. T. Nguyen and J. T. Hupp, *Chemical Society Reviews* **2009**, *38*, 1450-1459; d) Y. Li, H. Xu, S. Ouyang and J. Ye, *Physical Chemistry Chemical Physics* **2016**, *18*, 7563-7572; e) C.-C. Wang, J.-R. Li, X.-L. Lv, Y.-Q. Zhang and G. Guo, *Energy & Environmental Science* **2014**, *7*, 2831-2867.
- [3] a) N. A. Khan, Z. Hasan and S. H. Jhung, *Journal of hazardous materials* **2013**, *244*, 444-456; b) J.-R. Li, J. Sculley and H.-C. Zhou, *Chemical reviews* **2011**, *112*, 869-932; c) J. B. DeCoste and G. W. Peterson, *Chemical reviews* **2014**, *114*, 5695-5727; d) B. Van de Voorde, B. Bueken, J. Denayer and D. De Vos, *Chemical Society Reviews* **2014**, *43*, 5766-5788; e) S. A. A. Razavi, M. Y. Masoomi and A. Morsali, *Chemistry-A European Journal* **2017**, *23*, 12559-12564; f) S. A. A. Razavi, M. Y. Masoomi and A. Morsali, *Inorganic chemistry* **2017**, *56*, 9646-9652; g) S. A. A. Razavi, M. Y. Masoomi and A. J. I. c. Morsali, *Inorganic Chemistry* **2018**, *57*, 11578-11587.
- [4] a) K. Sumida, D. L. Rogow, J. A. Mason, T. M. McDonald, E. D. Bloch, Z. R. Herm, T.-H. Bae and J. R. Long, *Chemical reviews* **2011**, *112*, 724-781; b) Y. He, W. Zhou, G. Qian and B. Chen, *Chemical Society Reviews* **2014**, *43*, 5657-5678; c) L. J. Murray, M. Dincă and J. R. Long, *Chemical Society Reviews* **2009**, *38*, 1294-1314; d) S. A. A. Razavi, M. Y. Masoomi, T. Islamoglu, A. Morsali, Y. Xu, J. T. Hupp, O. K. Farha, J. Wang and P. C. Junk, *Inorganic Chemistry* **2017**, *56*, 2581-2588.
- [5] A. Morozan and F. Jaouen, *Energy & environmental science* **2012**, *5*, 9269-9290.
- [6] I. Imaz, M. Rubio-Martínez, J. An, I. Sole-Font, N. L. Rosi and D. Maspoch, *Chemical communications* **2011**, *47*, 7287-7302.
- [7] M. Kurmoo, *Chemical Society Reviews* **2009**, *38*, 1353-1379.
- [8] V. V. e. Butova, M. A. Soldatov, A. A. Guda, K. A. Lomachenko and C. Lamberti, *Russian Chemical Reviews* **2016**, *85*, 280.
- [9] J. H. Bang and K. S. Suslick, *Advanced Materials* **2010**, *22*, 1039-1059.
- [10] a) B. W. Zeiger and K. S. Suslick, *Journal of the American Chemical Society* **2011**, *133*, 14530-14533; b) V. Safarifard and A. Morsali, *Coordination Chemistry Reviews* **2015**, *292*, 1-14.
- [11] a) S. A. A. Razavi, M. Y. Masoomi and A. Morsali, *Ultrasonics Sonochemistry* **2017**, *37*, 502-508; b) S. A. A. Razavi, M. Y. Masoomi and A. Morsali, *Ultrasonics sonochemistry* **2018**, *41*, 17-26.
- [12] K. S. Suslick, *Science* **1990**, *247*, 1439.
- [13] K. S. Suslick, D. A. Hammerton and R. E. Cline, *Journal of the American Chemical Society* **1986**, *108*, 5641-5642.
- [14] O. Karagiari, W. Bury, J. E. Mondloch, J. T. Hupp and O. K. Farha, *Angewandte Chemie International Edition* **2014**, *53*, 4530-4540.
- [15] a) S. M. Cohen, *Chemical Reviews* **2012**, *112*, 970-1000; b) P. Deria, J. E. Mondloch, E. Tylianakis, P. Ghosh, W. Bury, R. Q. Snurr, J. T. Hupp and O. K. Farha, *Journal of the American Chemical Society* **2013**, *135*, 16801-16804.
- [16] M. Bagheri, M. Y. Masoomi and A. Morsali, *Sensors and Actuators B: Chemical* **2016**.
- [17] Y. Han, J.-R. Li, Y. Xie and G. Guo, *Chemical Society Reviews* **2014**, *43*, 5952-5981.

- [18] a) W. Bury, D. Fairen-Jimenez, M. B. Lalonde, R. Q. Snurr, O. K. Farha and J. T. Hupp, *Chemistry of Materials* **2013**, *25*, 739-744; b) O. Karagiari, W. Bury, E. Tylianakis, A. A. Sarjeant, J. T. Hupp and O. K. Farha, *Chemistry of Materials* **2013**, *25*, 3499-3503.
- [19] M. Y. Masoomi, A. Morsali and P. C. Junk, *CrystEngComm* **2015**, *17*, 686-692.